A MODEL OF THE VENUS IONOSPHERE

A. F. Nagy, S. C. Liu, T. M. Donahue and S. K. Atreya

Department of Atmospheric and Oceanic Science
The University of Michigan, Ann Arbor, Michigan 48104

P. M. Banks

Department of Applied Physics and Information Science
University of California, San Diego, La Jolla, California 92037

Abstract. Results of model calculations of the Venus ionosphere covering the altitude range from 120 km to 300 km are presented. The chemical scheme and the reaction rates adopted for the model are the same as given in a recent paper by Kumar and Hunten [1974], except that the electron temperature dependence of the dissociative recombination rates is taken into account. The calculations were carried out for 'low' and 'high' atomic oxygen models, corresponding to an $[O]/[CO_2]$ ratio of 0.4 percent and 4 percent respectively at 140 km. The results of the calculations agree well in both shape and magnitude with the Mariner 5 and 10 occultation results in the chemically controlled region; at the higher altitudes reasonable agreement with the observation is obtained if diffusive equilibrium and high vertical flow velocities (10 km/sec) are assumed as upper boundaries for the Mariner 5 and 10 conditions, respectively, although solar wind-ionosphere interactions are the likely controlling mechanism for the Mariner 10 case.

Introduction

The most recent published work on the Venus ionosphere is by Bauer and Hartle [1974], who presented a model which was successful in fitting the Mariner 10 ionospheric observations [Howard et al., 1974; Fjeldbo et al., 1975]. However, to obtain such an agreement the authors assumed that at 180 km the $[O]/[CO_2]$ ratio is sixty, a value that appears to be unacceptable according to a number of different and independent criteria. Such a high atomic oxygen density implies an optical depth for ionizing solar radiation, of about four at 150 km, due to atomic oxygen alone, which is inconsistent with the observation of an electron density peak at 145 km, if this peak is the F_1 maximum. This high $[O]/[CO_2]$ ratio is also much larger than the values deduced by Liu and Donahue [1975] and Sze and McElroy [1975] based on hydrogen balance considerations. Finally, the atomic oxygen value proposed by Bauer and Hartle [1974] implies an $[O]/[CO_2]$ ratio of two at 140 km, which is about an order of magnitude higher than even the value deduced from 1304 Å airglow measurements by Rottman and Moos [1973] and Strickland [1973], a value in itself far larger than that allowed by the hydrogen balance arguments.

The purpose of this letter is to outline an ionospheric model, which uses acceptable atomic oxygen density values and which is successful in reproducing the Mariner 5 and 10 observations below 200 km. First, we will briefly outline the neutral atmosphere model, reaction rate scheme, ion production rates and other relevant assumptions used in our calculations and will then present some representative results.

Model Assumptions

The CO_2 and O altitude profiles, used in our model calculations, were extrapolated values taken from Liu and Donahue [1975]; an exospheric temperature of 350°K was adopted, as suggested by Kumar and Hunten [1974]. In order to cover the possible range of atomic oxygen densities, calculations were carried out using both a 'high' and 'low' atomic oxygen model. The 'high' and 'low' models correspond to an $[O]/[CO_2]$ ratio of 4 percent and 0.4 percent, respectively at 140 km. The corresponding eddy coefficients are $10^7 cm^2 sec^{-1}$ and $10^8 cm^2 sec^{-1}$, respectively. The hydrogen and helium densities at 200 km were taken to be $5 \times 10^4 cm^{-3}$ [Sze and McElroy, 1975] and $1 \times 10^5 cm^{-3}$, respectively [Broadfoot et al., 1974].

We adopted the chemical model outlined by Kumar and Hunten [1974]. We also used the reaction rates tabulated by these authors, except for taking into account the electron temperature dependence of the dissociative recombination rate coefficients of O_2^+ and CO_2^+. The recent measurement of the O_2^+ recombination rate by Walls and Dunn [1974] give:

$$\alpha(O_2^+) = 8.75 \times 10^{-6}(T_e)^{-0.67} \quad 100°K \lesssim T_e \lesssim 3000°K$$

The best available estimate gives a T_e^{-1} variation for the dissociative recombination rates of CO_2^+ [Bauer, 1973]. Therefore the following relationship for $\alpha(CO_2^+)$ is obtained from the measured value at 300°K:

$$\alpha(CO_2^+) = 1.14 \times 10^{-4}(T_e)^{-1.0} \quad T_e \gtrsim 300°K$$

There is considerable controversy over the absolute magnitude of the solar EUV flux values, but recent, yet unpublished measurements with the EUV spectrophotometer on Atmospheric Explorer C indicates that the most recent flux value published by Hinteregger [1970] are appropriate for

LAST COPY

present solar cycle conditions [H. E. Hinteregger, private communications]. Thus, for the Mariner 10 ion production rate calculations we used the Hinteregger [1970] values, scaled for Venus, but for the Mariner 5 calculations the flux values were increased by a factor of 120/75, which is the ratio of the appropriate 10.7 cm flux values. The photoabsorption and ionization cross section were taken from the tabulations of Stewart and Webb [1963], Cook and Metzger [1964], Samson and Cairns [1965], Samson [1966], and Henry and McElroy [1968].

Numerical solutions of the following one-dimensional coupled continuity and momentum equations for O^+, O_2^+, CO_2^+, He^+, H^+ in the altitude region of 120 km to 300 km were obtained:

$$\frac{d}{dz}\phi_j = P_j - L_j \qquad (1)$$

$$\phi_j = -D_j n_j \left[\frac{1}{n_j}\frac{dn_j}{dz} + \frac{m_j g}{kT_I} + \frac{T_e/T_I}{n_e}\frac{dn_e}{dz} + \frac{1}{T_I}\frac{d(T_e + T_I)}{dz} \right] \qquad (2)$$

where P_j and L_j are respectively the production and loss rates of the jth species, ϕ_j is the flux, D_j is the diffusion coefficient, n_j is the density, n_e is the electron density, and T_I is the ion temperature. In the above formulation of the momentum equation the acceleration term and the neutral gas velocity are taken to be negligible, assumptions which appear to be reasonable for the Venus atmosphere. Chemical lifetimes are of the same order as diffusion lifetime at about 190 km, therefore the region below that altitude is controlled by photochemistry, while transport processes are dominant at the higher altitudes. In the numerical scheme photochemical equilibrium conditions were used as the lower boundary, while flux values were specified for the upper boundary conditions. The coupled energy equations were not solved in these calculations; the electron and ion temperature profiles were input parameters and will be discussed in the next section.

Results

The resutls of ionospheric model calculations corresponding to Mariner 5 conditions are shown in Figure 1, along with the measured electron density profile [Kliore et al., 1967]. The results of calculations for low neutral atomic oxygen are shown; the electron density peak is at an altitude of 140 km, in accordance with the observations. For high neutral atomic oxygen the profile of electron density if similar to that of low oxygen but with more O^+ and less CO_2^+. The calculated peak densities are $5 \times 10^5 cm^{-3}$ and $4.2 \times 10^5 cm^{-3}$ for the high and low oxygen models, respectively, which is to be compared to the measured value of $6 \times 10^5 cm^{-3}$. Before passing on to a discussion of the calculated densities at higher altitudes, it is appropriate to examine the low altitude results obtained for the

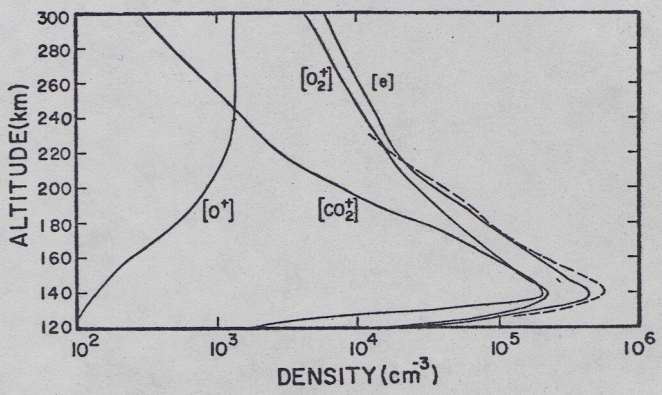

Figure 1. The calculated distributions of the major ions and electrons, corresponding to Mariner 5 solar conditions and diffusive equilibrium upper boundary conditions, are shown with solid lines. The broken line is the electron distribution deduced from the Mariner 5 occultation experiment [Kliore et al., 1967].

Mariner 10 conditions, shown in Figure 2. For this case the calculated electron peak is located at 145 km, while the measured peak is near 142 km with a density of $2.9 \times 10^5 cm^{-3}$ [Fjeldbo et al., 1975]. The calculated peak densities are $2.4 \times 10^5 cm^{-3}$ and $2.1 \times 10^5 cm^{-3}$ for the high and low oxygen models, respectively. Again we show the calculated ion densities for the low [O] case only. It should be noted that the major ion is O_2^+ up to about 290 km for all conditions presented in this paper.

The detailed variation of both the ion composition and ion density slopes above the peak depends strongly on the electron and ion temperatures, the vertical and horizontal flow velocities, and the interactions with the solar wind. More complex models involving coupled energy and multidimensional solutions may advance our understanding of the temperature and flow conditions, even without any new experimental data base. We are proceeding with such model calculations; however they are extremely complex and no results are expected in the very near future, therefore the results presented here, based on certain assumptions, have to await later judgement.

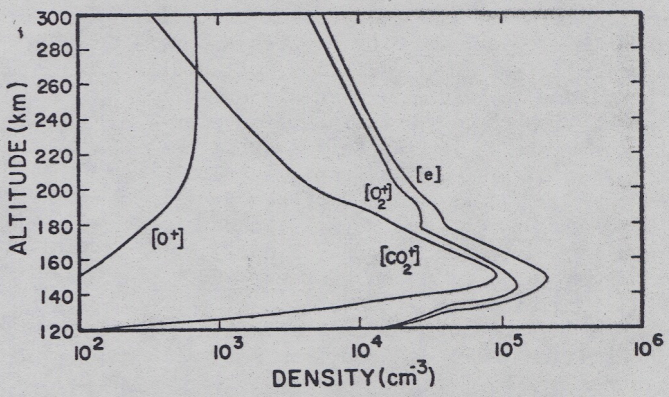

Figure 2. The calculated distributions of the major ion species and electrons, corresponding to Mariner 10 solar conditions and diffusive equilibrium upper boundary conditions, are shown with solid lines.

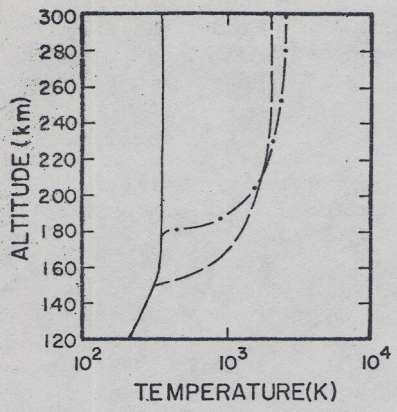

Figure 3. The neutral gas and ion temperatures used in the calculations are shown by the solid line. The electron temperatures assumed for the Mariner 5 and 10 conditions are shown by the dashed and dot-dashed lines, respectively.

There are no direct experimental data on electron and/or ion temperatures in the Venus ionosphere. Theoretical calculations by Herman et al. [1971] give electron temperature values which depart very rapidly from the neutral temperature values as the altitude increases, beginning at about 145 km, with gradients of the order of 30°K km^{-1}. Electron temperatures in the terrestrial ionosphere exhibit similar characteristics. The Mariner 10 electron density measurements [Howard et al., 1974; Fjeldbo et al., 1975] indicate the presence of a pronounced ledge near 180 km. Our model reproduces the observed ledge (see Figure 2) if the electron temperature is made to increase from the neutral temperature value of 350°K at 178 km to about 900°K at 188 km. Such a temperature variation does not appear to be unreasonable when compared with the model of Herman et al. [1971] or terrestrial conditions. The corresponding heat flow, of the order of 2.5×10^9 eV $cm^{-2}sec^{-1}$, is not extraordinarily large. These test calculations combined with the lack of experimental data, led us to adopt an electron and ion temperature profile, as shown in Figure 3.

The Mariner 5 electron density profile shows no pronounced ledge near 180 km. If the Mariner 10 ledge is due to electron temperature variation, as discussed above, then the relevant conditions must have been different during the two flybys. The Mariner 5 observations [Kliore et al., 1967] were made near solar cycle maximum conditions and a solar zenith angle of 33°. Terrestrial ionospheric data indicate that in general the electron temperatures are lower during solar cycle maximum conditions and significant departures from the neutral temperature values take place at lower altitudes with decreasing solar zenith angles, which led us to adopt the temperature profile shown in Figure 3. We have carried out numerous calculations with different temperature profiles and while the details of specific features (e.g., the ledge) do depend on the temperatures chosen, the overall results and conclusions are not very sensitive to temperature variations within reasonable bounds.

The upper boundary conditions at 300 km do not affect the solutions below about 185 km, but have a strong control over the density magnitudes and slopes in the upper regions. The calculations plotted in Figure 1 for Mariner 5 were obtained by assuming a zero flux (diffusive equilibrium) upper boundary condition and the fit with the measured data is reasonably good. The Mariner 5 measurements indicated an ionopause at an altitude of about 500 km, thus the influence of the solar wind should be negligible at 300 km; therefore the presence of diffusive equilibrium conditions at 300 km appears to be a reasonable assumption. The use of zero flux upper boundary condition for the Mariner 10 case, on the other hand, leads to a drastic disagreement with the occultation data. THe Mariner 10 observations showed an ionopause near 340 km, which implies the presence of strong solar wind-ionsosphere interactions in this altitude region. Bauer and Hartle [1974] have succeeded in reproducing the observed electron density profile above 200 km, by considering compression due to downward transport caused by solar wind interaction. We can also get reasonable agreement with the data by assuming an upward flow of 10 km/sec at 300 km as shown in Figure 4. The ionosphere observed by Mariner 10 corresponds to a solar zenith angle of 67.1°, and there should be significant horizontal and vertical velocities present in the upper ionosphere due to both plasma transport from the subsolar to antisolar regions and the momentum transfer from the solar wind to the ionospheric plasma. Nevertheless, the vertical velocities needed to reproduce the observations appear to be unreasonably high and the compression mechanism suggested by Bauer and Hartle [1974] seem more realistic at this time. An increased data base and/or multidimensional calculations are needed to shed more light on the mechanisms controlling the topside ionosphere. Finally, it should be pointed out that the data reduction scheme used with the radio occultation experiment assumed spherical symmetry for the ionosphere, which could introduce spurious results at the higher altitude if the ionosphere is truly highly nonsymmetric near the terminator.

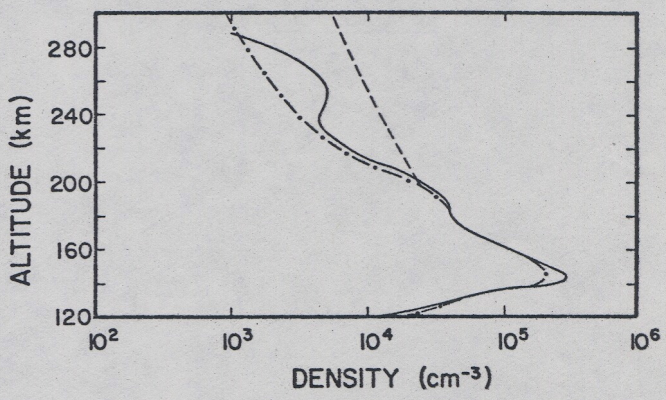

Figure 4. A comparison of the calculated electron density profiles calculated corresponding to the Mariner 10 solar conditions; the dashed curve shows the results obtained for diffusive equilibrium condition while the dot-dashed curve corresponds to an upward flow velocity of 10 km/sec at 300 km. The measured densities [Howard et al., 1974] are shown by the solid curve.

In summary we have presented an ionospheric model for Venus, which is based on the best available estimates on neutral gas parameters, reaction rates and temperatures. The calculated densities are in reasonably good agreement with the observed values below 200 km. An assumption of zero vertical velocity at the 300 km upper boundary leads to agreement between the calculations and Mariner 5 measurements, but no such agreement is achieved for the Mariner 10 case, where solar wind-ionosphere interaction is likely to control the behavior of the topside ionosphere. The major outstanding problems appear to be the nature of the electron and ion temperature variations, the plasma flow velocities and the nature of the solar wind-ionosphere interaction. Meaningful progress in the first two of these topics is possible, even without new experimental data, with more complex multidimensional models which also include the solution of the coupled energy equations. We have started such model calculations and will report on them as soon as we have obtained meaningful results.

Acknowledgements. This work was supported in part by the National Aeronautics and Space Administration under grants NGR-05-009-075 at The University of California, San Diego and NGR-23-005-015 and DES-74-21598 at The University of Michigan.

References

Bauer, S. J., Physics of Planetary Ionospheres, ed. J. G. Roederer, p. 85, Springer-Verlag, New York, 1973.

Bauer, S. J. and R. E. Hartle, Venus ionosphere: An interpretation of Mariner 10 observations, Geophys. Res. Lett., 1, 7, 1974.

Broadfoot, A. L., S. Kumar, M.J.S. Belton, and M. B. McElroy, Ultraviolet observations of Venus from Mariner 10, Science, 183, 1315, 1974.

Cook, G. R. and P. H. Metzger, Photoionization and absorption cross section of H_2 and D_2 in the vacuum ultraviolet region, J. Opt. Soc. Amer., 54, 968, 1964.

Fjeldbo, G. B. Seidel, and D. Sweetnam, The Mariner 10 radio occultation measurements of the ionosphere of Venus, J. Atmos. Sci., in press, 1975.

Henry, R.J.W. and M. B. McElroy, Photoelectrons in planetary atmospheres, in The Atmospheres of Venus and Mars, ed. J. C. Brandt and M. B. McElroy, p. 251, Gordon and Breach, New York, 1968.

Herman, J. R., R. E. Hartle, and S. J. Bauer, The dayside ionosphere of Venus, Planet. Space Sci., 19, 443, 1971.

Hinteregger, H. E., The extreme ultraviolet solar spectrum and its variation during solar cycle, Ann. Geophys., 26, 547, 1970.

Howard, H. T., et al., Venus: Mass gravity field, atmosphere, and ionosphere as measured by the Mariner 10 dual frequency radio system, Science, 183, 1297, 1974.

Kliore, A. J., G. S. Levy, D. L. Cain, G. Fjeldbo, and S. I. Rasool, Atmosphere and ionosphere of Venus from Mariner 5 S-band radio occultation experiment, Science, 158, 1683, 1967.

Kumar, S. and D. M. Hunten, Venus: An ionospheric model with an exospheric temperature of 350°K, J. Geophys. Res., 79, 2529, 1974.

Liu, S. C. and T. M. Donahue, The aeronomy of the upper atmosphere of Venus, Icarus, in press, 1975.

Rottman, E. J. and A. W. Moos, The ultraviolet (1200-1900 Angstrom) spectrum of Venus, J. Geophys. Res., 78, 8033, 1973.

Samson, J.A.R., The measurement of the photoionization cross-sections of the atomic gases, in Advances in Atomic and Molecular Physics, Vol. 2, p. 177, Academic Press, New York, 1966.

Samson, J.A.R. and R. B. Cairns, Total absorption cross-sections of H_2, N_2 and O_2 in the region 550-200 Å, J. Opt. Soc. Amer., 55, 1035, 1965.

Stewart, A. L. and T. G. Webb, Photoionization of helium and ionized lithium, Proc. Phys. Soc. (London), 82, 532, 1963.

Strickland, D. J., The OI1304 and 1356 Å emissions from the atmosphere of Venus, J. Geophys. Res., 78, 2827, 1973.

Sze, D. N. and M. B. McElroy, Some problems in Venus aeronomy, Planet. Space Sci., in press, 1975.

Walls, F. L. and G. H. Dunn, Measurement of total cross-sections for electron recombination with NO^+ and O_2 using ion storage techniques, J. Geophys. Res., 79, 1911, 1974.

(Received December 16, 1974;
revised January 17, 1975;
accepted February 3, 1975.)